electronic, then we would replace the values in the first column of Table I by 1.43, 2.2, 9.4, and 360, respectively, from top to bottom. This alteration would not change appreciably any of our other conclusions.

[13]F. J. McClung, Hughes Research Laboratory, Report No. 306 (unpublished).

[14]J. P. Jesson and H. W. Thompson, Proc. Roy. Soc. (London) A268, 68 (1962).

[15]R. W. Hellwarth (unpublished).

[16]R. W. Hellwarth, J. Chem. Phys. 52, 2128 (1970).

[17]S. P. S. Porto (private communication).

PHYSICAL REVIEW B VOLUME 5, NUMBER 2 15 JANUARY 1972

Polarization of Luminescence in NaCl : Pb^{2+} and KCl : Pb^{2+} †

W. C. Collins* and J. H. Crawford, Jr.

Physics Department, University of North Carolina, Chapel Hill, North Carolina 27514

(Received 3 September 1971)

The polarized luminescence of Pb^{2+} impurity-vacancy complexes in NaCl and KCl induced by excitation with polarized light has been studied. A single emission band at 340 nm of predominantly tetragonal symmetry was found in KCl : Pb; this emission decreased and shifted in wavelength during aging. Three emission bands were found in NaCl : Pb at 315, 380, and 460 nm. The 315-nm emission was at its maximum intensity after quenching and the 380-nm band was the first to appear upon aging with the 460-nm band appearing later. The 315-nm emission was found to originate from centers of both tetragonal and orthorhombic symmetry. Both the 380- and 460-nm bands are due to centers of trigonal symmetry. We have assigned the 340-nm band in quenched KCl and the 315-nm band in NaCl to isolated Pb-vacancy dipoles. We conclude that in KCl the vacancies are predominantly next-nearest neighbors to the impurity while in NaCl both nearest- and next-nearest-neighbor sites are comparable. The 380-nm emission band appears to be due to trimers of dipoles in a hexagon arrangement in {111} plane in agreement with the model of Dryden and Harvey. That the origin of the 460-nm band is due to higher aggregates is not well established.

I. INTRODUCTION

The state of dispersion of divalent impurities in the alkali halides has been of considerable interest in color-center research.[1] At ordinary temperatures these impurities are bound to the charge-compensating vacancies forming dipolar complexes, and the role of the vacancies in the observed properties of the complexes is not yet fully understood. This is particularly true regarding the aggregation of impurities. Cook and Dryden[2] first measured the aggregation of divalent impurity-cation vacancy complexes by observing the kinetics of the decay of dielectric loss. They observed an initial third-order reaction and proposed that three dipoles combine simultaneously forming a trimer of dipoles in a hexagonal arrangement in the {111} plane as the first stage of aggregation. They postulated that further aggregation consists of the addition of dipoles, two at a time, to the trimers forming pentamers, heptamers, etc. all in the {111} plane.

It has long been known that the luminescent emission of the Pb ions in the alkali halides is sensitive to the state of dispersion of the ions.[3] In general s^2-configuration ions, such as Pb^{2+}, exhibit three characteristic absorption bands in the ultraviolet designated A, B, and C in the order of increasing energy.[4] Seitz[5] has attributed these to the intraionic transitions $s^2 \rightarrow sp$, or $a_{1g}^2 \rightarrow a_{1g}t_{1u}$ in the molecular-orbital description of Sugano.[6] The C band corresponds to the dipole-allowed transition $^1S_0 \rightarrow {}^1P_1 \times (A_{1g} \rightarrow T_{1u})$; the B band corresponds to the vibration-induced transition $^1S_0 \rightarrow {}^3P_2 (A_{1g} \rightarrow E_u, T_{2u})$; and the A band corresponds to the spin-orbit-allowed transition $^1S_0 \rightarrow {}^3P_1 (A_{1g} \rightarrow T_{1u})$. Excitation in the Pb^{2+}-A band leads to a 340-nm emission in KCl and three emission bands in NaCl at 315, 380, and 460 nm. The 340-nm band in KCl and the 315-nm band in NaCl are at a maximum upon quenching with the 380- and 460-nm bands in NaCl appearing successively upon aging. Dryden and Harvey[7] assigned these emission bands to particular aggregates in NaCl by comparing their decay and growth with the expected behavior of monomers, trimers, pentamers, etc. according to the Cook and Dryden model.[2] They assigned the 315-nm band to monomers, the 380-nm band to trimers and the 460-nm band to heptamers. None of the emission bands could be correlated with the expected behavior of pentamers.

The polarization properties of the emission bands of the s^2 ions have also received considerable attention. Klick and Compton[8] first measured the polarization of the luminescence of KCl : Tl at low tem-

perature. Lushchik[9] and Zazubovich[10] carried out extensive studies of the polarization characteristics of many s^2 ions (Ga^+, Ge^{+2}, In^+, Sn^{+2}, Tl^+, Pb^{+2}, Bi^{+3} in KCl and Sn^{+2} in KCl, KBr, and KI) in the alkali halides. Most of the monovalent ions showed polarized emission only at low temperature while the divalent and trivalent ions had polarized emission up to and above room temperature. In every case the symmetry axis of the anisotropic centers were tetragonal, and the maximum degree of polarization was considerably less than unity. Zazubovich[10] speculated on the causes of the low symmetry in these emission centers. He considered static causes such as perturbations by nearby vacancies or preferential bonding to the halide ions as more important than dynamic causes such as the dynamic Jahn-Teller effect. Koeze and Volger[11] measured the polarized emission of the Pb^{+2} luminescent center in KCl, and they attributed the observed tetragonal symmetry to vacancies in the next-nearest-neighbor position. They considered the A band to be a doublet corresponding to transitions with opposite polarization character. The large overlapping of the two bands would then be the origin of the large depolarization observed. Fukuda[12] *et al.* investigated the polarization characteristics of several monovalent and divalent s^2 ions (Ga^+, In^+, Sn^{+2}, Tl^+, Pb^{+2}) in KBr at liquid-nitrogen and liquid-helium temperature as well as at room temperature. His results agree with the other investigators. Fukuda, however, attributed the low symmetry to interactions with the nontotally symmetric lattice vibrations around the center, i.e., the dynamic Jahn-Teller effect. The model presented was based on the very extensive theoretical work of Toyozawa and Inoue[13] and the earlier work of Kamimura and Sugano[6] on the electron-lattice interactions of s^2 ions in the alkali halides. The model presented by Fukuda gives a qualitative explanation for some of the polarization properties reported. This has been extended recently to include the possible effects of nearby vacancy and has been used to explain the polarization characteristics of KI:Sn^{+2}.[14] The model fits the data only if it is assumed that the vacancy is in the nearest-neighbor position. In this study the polarized emission of Pb^{2+} ions in NaCl and KCl are investigated with emphasis on the role played by the charge-compensating cation vacancies. The exciting light in the Pb^{2+}-A band was incident in the ⟨100⟩ (or ⟨110⟩) direction and, in order to investigate various possible symmetries, the polarization of luminescence was measured for light emitted parallel to this direction and in a ⟨100⟩ (or ⟨110⟩) direction perpendicular to it. This observational arrangement is shown in Figs. 1 and 2. Table I gives the expected azimuthal dependence of polarization in the parallel configuration for ⟨100⟩ and ⟨110⟩ cut crystals.[15] Table II gives the expected polarization diagrams in the perpendicular configuration for ⟨100⟩ and ⟨110⟩ cut crystals.

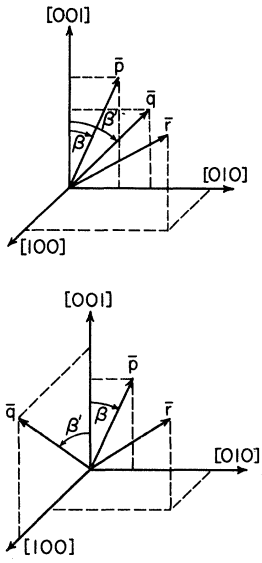

FIG. 1. Crystal orientations for excitation and observation in ⟨100⟩ directions. The electric vectors for the exciting and emitted light are denoted $\bar{p}$ and $\bar{q}$, respectively, while $\bar{r}$ lies along the symmetry axis of the relevant center. The upper diagram represents the parallel configuration with $\bar{p} = [0, \sin\beta, \cos\beta]$, $\bar{g} = [0, \sin\beta', \cos\beta']$, $\bar{r} = [h, k, l]$. The lower diagram represents the perpendicular configuration with $\bar{p} = [0, \sin\beta, \cos\beta]$, $\bar{q} = [\cos\beta', 0, \sin\beta']$.

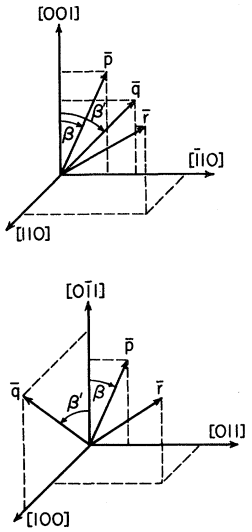

FIG. 2. Crystal orientations for excitation in the ⟨100⟩ or ⟨110⟩ directions and observation in the ⟨110⟩ direction. The upper diagram represents the parallel configuration with $\bar{p} = [\sin(\beta/\sqrt{2}), \sin(\beta/\sqrt{2}), \cos\beta]$, $\bar{q} = [\sin(\pi'/\sqrt{2}), \sin(\beta'/\sqrt{2}), \cos\beta']$. The lower diagram represents the perpendicular configuration with $\bar{p} = [0, \sin(\beta - \frac{1}{4}\pi), \cos(\beta - \frac{1}{4}\pi)]$, $\bar{q} = [\cos\beta', -\sin(\beta'/\sqrt{2}), \sin(\beta'/\sqrt{2})]$.

II. EXPERIMENTAL

Two experimental arrangements (Fig. 3) were necessary for the measurements described above. Since the parallel configuration was sensitive to scattered light it was essential that a double monochromator be used for excitation. The scattered light in the Leiss double monochromator which was used was less than 10^{-5}. The Bausch and Lomb 500-mm monochromator was used for excitation in the perpendicular configuration. For both configurations, either a Bausch and Lomb 250-mm monochromator or a set of narrow-band isolation filters were used to observe the emission. The polarizers and analyzers were Polaroid HNP'B filters, the

TABLE I. Azimuthal dependence of polarization defined by $P(\alpha)=(I_{\parallel}-I_{\perp})/(I_{\parallel}+I_{\perp})$, where $I_{\parallel}$ and $I_{\perp}$ refer to $\beta=\beta'=\alpha$ and $\beta=\beta'+90°=\alpha$, respectively. Here π and σ refer to transition moments of excitation or emission being parallel or perpendicular, respectively, to the center's symmetry axis denoted by C_2, C_3, or C_4.

		[100]	[110]
	$\pi-\pi$	$\frac{1+\cos4\alpha}{2}$	$\frac{3+2\cos2\alpha+3\cos4\alpha}{3+\cos2\alpha}$
C_4	$\sigma-\sigma$	$\frac{1+\cos4\alpha}{6}$	$\frac{3+2\cos2\alpha+3\cos4\alpha}{19+\cos2\alpha}$
	$\pi-\sigma$ $\sigma-\pi$	$-\frac{1+\cos4\alpha}{2}$	$-\frac{3+2\cos2\alpha+3\cos4\alpha}{2(5-\cos2\alpha)}$
	$\pi-\pi$	$\frac{1-\cos4\alpha}{2}$	$\frac{5-2\cos2\alpha-3\cos4\alpha}{2(5-\cos2\alpha)}$
C_3	$\sigma-\sigma$	$\frac{1-\cos4\alpha}{16}$	$\frac{5-2\cos2\alpha-3\cos4\alpha}{29-\cos2\alpha}$
	$\pi-\sigma$ $\sigma-\pi$	$-\frac{1-\cos4\alpha}{4}$	$-\frac{5-2\cos2\alpha-3\cos4\alpha}{2(7+\cos2\alpha)}$
	$\pi-\pi$	$\frac{3-\cos4\alpha}{6}$	$\frac{13-2\cos2\alpha-3\cos4\alpha}{2(13-\cos2\alpha)}$
C_2	$\sigma-\sigma$	$\frac{3-\cos4\alpha}{22}$	$\frac{13-2\cos2\alpha-3\cos4\alpha}{77-\cos2\alpha}$
	$\pi-\sigma$ $\sigma-\pi$	$-\frac{3-\cos4\alpha}{10}$	$\frac{13-2\cos2\alpha-3\cos4\alpha}{2(19+\cos2\alpha)}$

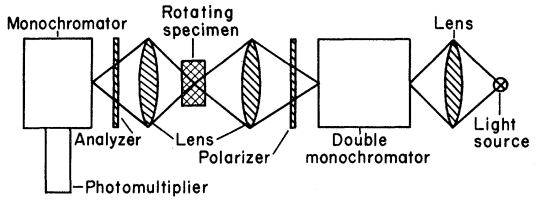

A. PARALLEL CONFIGURATION

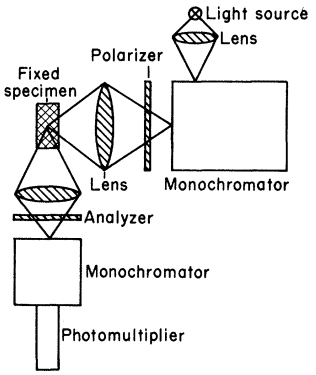

B. PERPENDICULAR CONFIGURATION

FIG. 3. Two experimental arrangements for measuring polarization.

light source was a high pressure Hg or D_2 lamp and the detector was an RCA 6199 or C70114J photomultiplier. For the parallel configuration the crystal was rotated in a plane perpendicular to the direction of propagation of the exciting light, and in the perpendicular configuration the crystal was held fixed and the polarizer rotated. The instrument polarization was corrected for by averaging the data between 180-deg rotations of the polarizer.

III. EXPERIMENTAL RESULTS

A. NaCl : Pb

Upon exciting the A band of the Pb ion, at liquid-nitrogen temperature (LNT), emission is observed at 315, 380, and 460 nm as shown in Fig. 4. The relative intensity of the emission bands is a sensitive function of thermal history and Pb concentration of the crystal. The 380-nm band is very weak at room temperature (RT), appearing as a hump on the shoulder of either the 315- or 460-nm band. At LNT it is larger by nearly an order of magnitude and is fully resolved, while the 315- and 460-nm bands increase by factors of 3 and 1.5, respectively. The 315-nm emission is at its maximum intensity immediately after quenching the crystal from 200 °C or higher, while the 380-nm band is at least an order of magnitude smaller, depending upon the effectiveness of quenching. The 460-nm band is not observed at all after this treatment. After annealing at RT or above, the long-wavelength bands in-

TABLE II. Polarization diagrams defined by $P(\beta)=(I_{\parallel}-I_{\perp})/(I_{\parallel}+I_{\perp})$, where $I_{\parallel}$ and $I_{\perp}$ refer to $\beta'=0°$ and 90°, respectively.

		[100] – [010]	[100] – [110]
	$\pi-\pi$	1	1
C_4	$\sigma-\sigma$	$\frac{1+\cos2\beta}{5+\cos2\beta}$	$\frac{1}{5}$
	$\pi-\sigma$ $\sigma-\pi$	$-\frac{1+\cos2\beta}{3-\cos2\beta}$	$-\frac{1}{3}$
	$\pi-\pi$	0	$\frac{\cos2\beta}{2+\cos2\beta}$
C_3	$\sigma-\sigma$	0	$\frac{\cos2\beta}{8+\cos2\beta}$
	$\pi-\sigma$ $\sigma-\pi$	0	$-\frac{\cos2\beta}{4-\cos2\beta}$
	$\pi-\pi$	$\frac{1+\cos2\beta}{5+\cos2\beta}$	$\frac{1+2\cos2\beta}{5+2\cos2\beta}$
C_2	$\sigma-\sigma$	$\frac{1+\cos2\beta}{21+\cos2\beta}$	$\frac{1+2\cos2\beta}{21+2\cos2\beta}$
	$\pi-\sigma$ $\sigma-\pi$	$-\frac{1+\cos2\beta}{11-\cos2\beta}$	$-\frac{1+2\cos2\beta}{11-2\cos2\beta}$

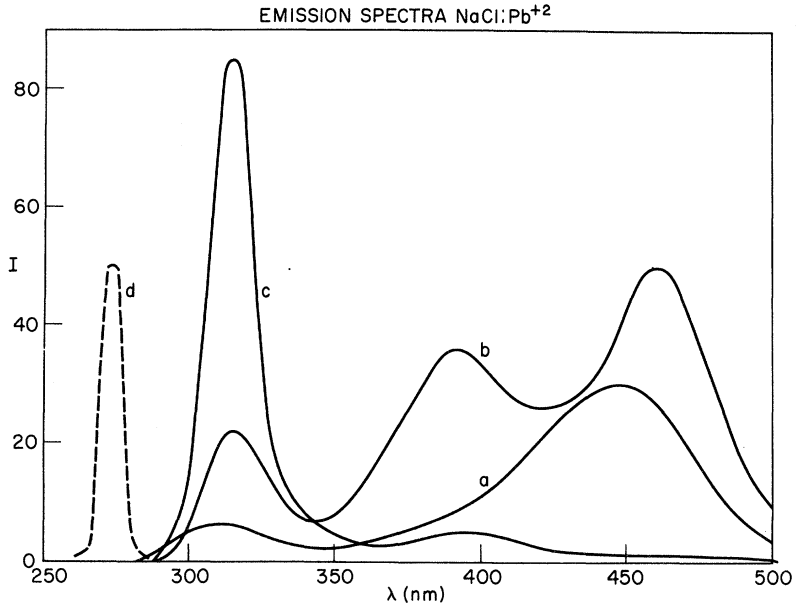

FIG. 4. Emission spectra for NaCl: Pb^{2+}: (a) aged crystal at RT, (b) aged crystal at LNT, (c) quenched crystal at LNT, (d) excitation.

crease at the expense of the 315-nm emission. The appearance of a large-460-nm-emission band in aged crystals was not universally observed. In NaCl : Pb (1000 ppm) grown locally, the 460-nm band was always weak while the other bands were intense. Similar results were observed in dilute NaCl : Pb (10 ppm) obtained from Harshaw Chemical Company.

The absorption spectrum at RT before and after quenching from 300 °C is shown in Fig. 5. In the prequench case a poorly resolved band appears on the low-energy side of the *A* band at above 290 nm. There is also considerable absorption on the low-energy side of the *C* band. After quenching the 290-nm band vanishes and the *A* band is greatly enhanced. The absorption on the low-energy side of the *C* band is also reduced. The prequench spectrum can be restored after prolonged aging at or slightly above RT.

The 315-nm emission is excited only by light falling in the *A* band, and its intensity decreases to zero rapidly for exciting light in the wings, even in well-aged crystals. The 380-nm emission is also principally excited in the *A* band but falls to zero much more gradually on the low-energy side. The 380-nm excitation spectrum mirrors closely the absorption in the *A*-band region for the prequenched specimen of Fig. 5. The 460-nm luminescence is also primarily excited in the central region of the *A* band similar to the 315-nm emission but in addition has a minor excitation band (unresolved in absorption) at 286 nm.

The polarization characteristics of each of the emission bands were investigated at both RT and LNT after various heat treatments. Each of the emission bands is partially polarized (~10 to 25%) at both RT and LNT. The degree of polarization was found to be independent of the emission wavelength across any given band, but the dependence on excitation wavelength across the *A* band was strong. Although the polarization spectra of the 380- and 460-nm bands are similar, these differ considerably from the behavior of the 315-nm band which is shown in Fig. 6 for excitation at LNT and observation in the ⟨100⟩ crystal direction (the parallel configuration illustrated in Fig. 1). At RT the excitation band is broader and the maximum degree of polarization is reduced by a factor of about 2 but

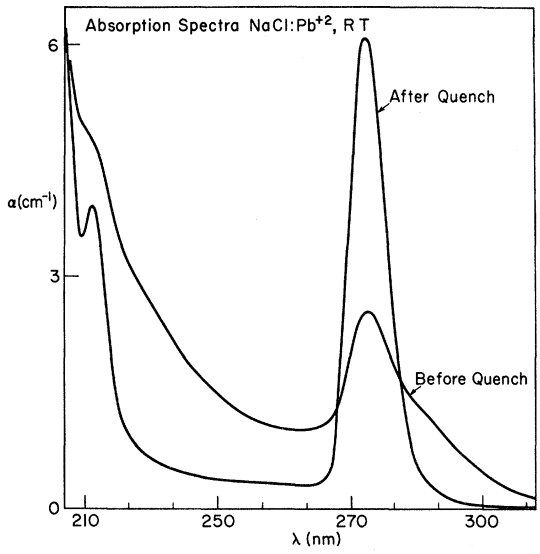

FIG. 5. Absorption spectra for NaCl : Pb^{2+} at RT.

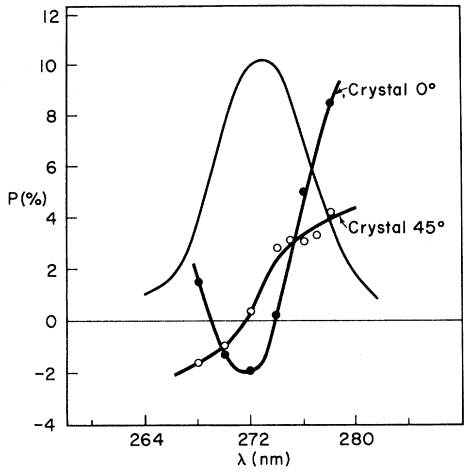

FIG. 6. Polarization and excitation spectra for the 315-nm emission at LNT in NaCl : Pb^{2+}.

the form of the spectrum remains the same. Figure 6 includes spectra for the crystal oriented both 0° and 45° with respect to the direction of polarization of exciting light. From this it can be seen that there exist three distinct regions of excitation across the A band. The maximum polarization for 0° azimuth occurs in the wings of the A band while the 45° azimuth gives a maximum in the center. Figure 7 shows the azimuthal dependence of the polarization for three selected wavelengths in each of the respective regions. Curves A, B, and C correspond to exciting wavelengths of 280, 265, and 272 nm, respectively. The experimental data are indicated by circles while the solid curves are of the form $a \pm b\,(1 + \cos 4\alpha)$ with the plus sign for the wings of the A band and the minus sign for the center. According to the table of azimuthal dependence (Table I) this best agrees with $\pi - \pi$ or $\sigma - \sigma$ transitions for tetragonal centers in the case of the A-band wings and $\pi - \sigma$ or $\sigma - \pi$ transition for tetragonal centers in the case of excitation at the peak of the A band. The expected azimuthal dependence from the Table is $\pm \frac{1}{2}(1 + \cos 4\alpha)$. Thus the observed degree of polarization appears to be much reduced and shifted relative to zero, but the angular dependence for tetragonal oscillators is clearly revealed.

The complexity of the polarization characteristics of the 315-nm emission makes impossible a simple explanation solely in terms of tetragonal oscillators without additional information. An examination of Table I reveals that the azimuthal dependence of polarization for the orthorhombic, trigonal, and tetragonal oscillators only differs in phase by 90° if we ignore the magnitude and shifts on the vertical axis. Thus a mixture of symmetries would still give an undistorted sinusoidal variation for the dominant species but would be reduced in magnitude and possibly shifted relative to zero. In order to distinguish between the possible symmetries, the perpendicular configuration shown in Fig. 2 was used. Table II shows that tetragonal oscillators have a constant polarization independent of β as distinguished from trigonal or orthorhombic. The experimental results are shown in Fig. 8 at both RT and LNT where the solid curves are plots of the function from the Table corresponding to orthorhombic centers. The close fit suggests the presence of centers of this symmetry while the large shifts from zero may well be due to contributions from centers of tetragonal symmetry.

The polarization spectra at LNT for the 380- and 460-nm bands are shown in Figs. 9 and 10. The increase in polarization upon cooling from RT and LNT is only about 20% for these bands. For 45° crystal azimuth the polarization degree has its maximum on the low-energy side of the A band while on the high-energy side it goes negative. The 0° azimuth is essentially constant across the excitation bands. Thus only two distinct regions of polarization exist. Figure 11 gives the azimuthal dependence of the polarization degree for the 380-nm band for selected wavelengths on the low- and high-energy side of the A band. The experimental data are circled while the solid curves are of the form $a \pm b\,(1 - \cos 4\alpha)$ with the plus and minus signs corresponding to excitation on the low- and high-energy sides of the A band, respectively. The azimuthal dependence of the polarization degree for the 460-nm emission band behaves in the same way. Consulting the Table of azimuthal dependences (Table I) again, we see that for $\pi - \pi$ or $\sigma - \sigma$ transitions of trigonal oscillators we have the expression $\frac{1}{2}(1 - \cos 4\alpha)$, while for the $\pi - \sigma$ or $\sigma - \pi$ transitions we have

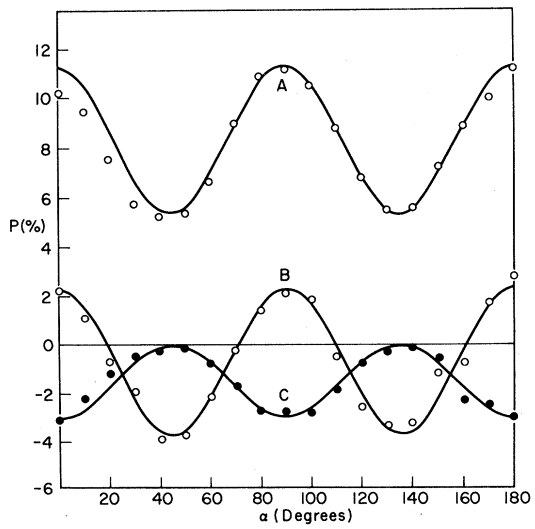

FIG. 7. Azimuthal dependence of polarization for the 315-nm emission at LNT in NaCl : Pb^{2+}.

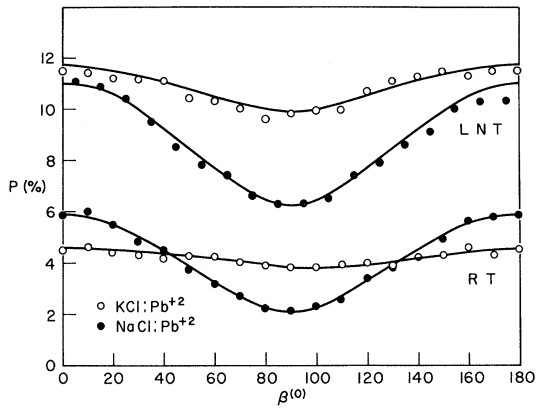

FIG. 8. Polarization diagrams for KCl and NaCl with excitation along [100] and observation along [011].

$-\frac{1}{4}(1-\cos 4\alpha)$. Thus it appears that the 380- and 460-nm emission centers are oriented along the crystal ⟨111⟩ axis. Again the absolute degree of polarization is greatly reduced but is not significantly shifted to zero. Examination of Table I reveals that orthorhombic oscillators have similar functional forms of azimuthal variation as trigonal, but they differ in degree and displacement from zero. This characteristic provides a strong argument for trigonal over orthorhombic.

Further evidence for the trigonal symmetry of the 380- and 460-nm bands is obtained by observing the azimuthal dependence of polarization for ⟨110⟩ cut crystals. A typical result is shown in Fig. 12 for the 380-nm band. Again the solid curves represent the functions for trigonal oscillators as given by Table I. Going one step further and using ⟨110⟩ cut crystals in the perpendicular configuration we can obtain the multipole order of the transition. Figure 13 is the resulting polarization diagram for the 460-nm emission for excitation on the high- and low-energy side of the A band. Again the solid curves are for trigonal oscillators but now we can distinguish between $\pi-\pi$ or $\sigma-\sigma$ transitions. The dotted curve is the best fit for the $\pi-\pi$ transition, while the solid curve corresponds to the $\sigma-\sigma$ transition. We require that all curves go through $P=0$

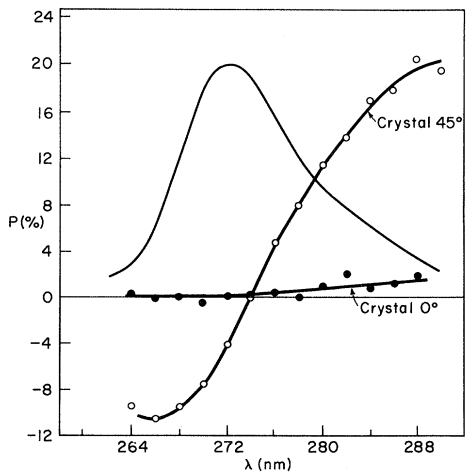

FIG. 9. Polarization and excitation spectra for the 380-nm emission at LNT in NaCl : Pb^{2+}.

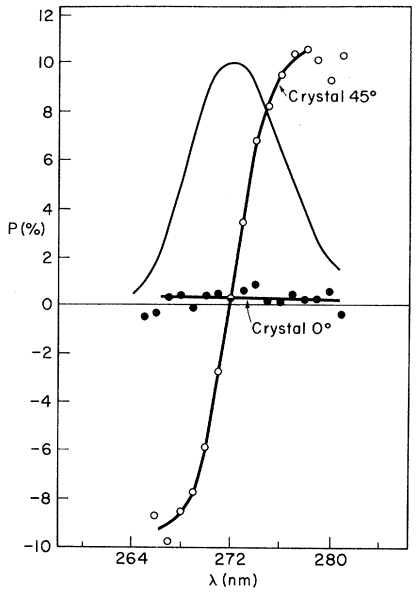

FIG. 10. Polarization and excitation spectra for the 460-nm emission at LNT in NaCl : Pb^{2+}.

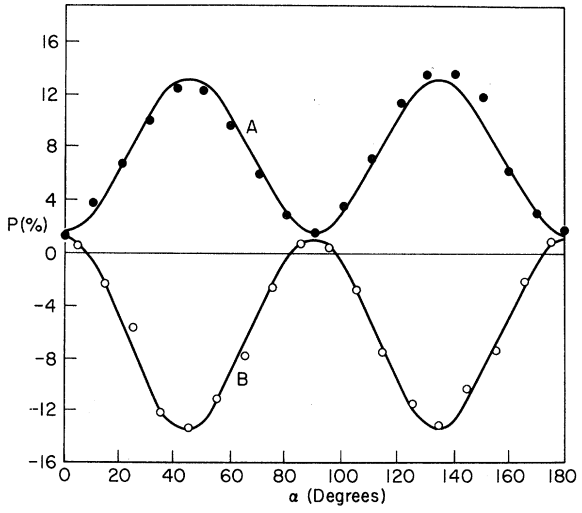

FIG. 11. Azimuthal dependence of polarization for the 380-nm emission in ⟨100⟩ cut NaCl : Pb^{2+}. A and B correspond to excitation on the low- and high-energy side of A band.

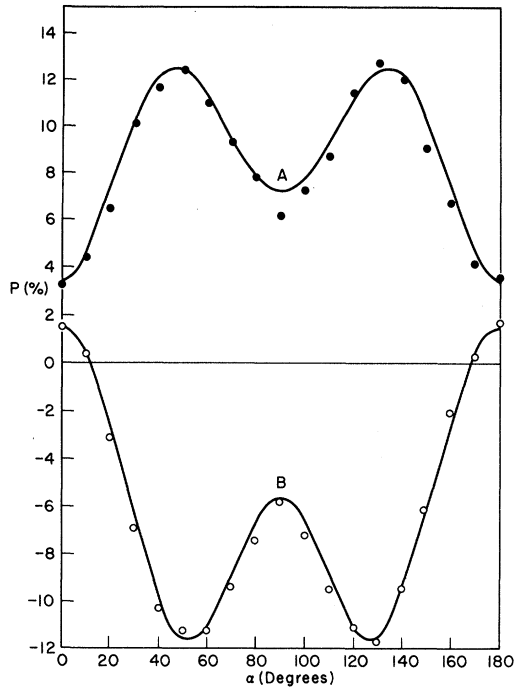

FIG. 12. Azimuthal dependence of polarization for the 380-nm emission in ⟨110⟩ cut NaCl : Pb^{2+}. *A* and *B* correspond to excitation on the low- and high-energy side of the *A* band.

for $\beta = 45°$. It thus appears that the relevant transitions for the low-energy excitation are $\sigma - \sigma$ and not $\pi - \pi$.

B. KCl : Pb^{++}

Excitation into the Pb-*A* band of KCl : Pb produces luminescence at 340 nm in freshly quenched crystals. In samples containing a few hundred ppm Pb^{2+} aging at or above RT leads to a decrease in the intensity of this band by approximately 50% and a shift in wavelength to 355 nm. The absorption spectrum is similar to NaCl : Pb but, unlike the case of NaCl, it is not sensitive to thermal history. Of course for these high-concentration crystals the optical density is so large that only the wings of the *A* band can be observed. Thus only in dilute KCl : Pb crystals was the *A* band measured as a function of thermal history, and in these there was no change, which is in marked contrast to observations on dilute NaCl : Pb.

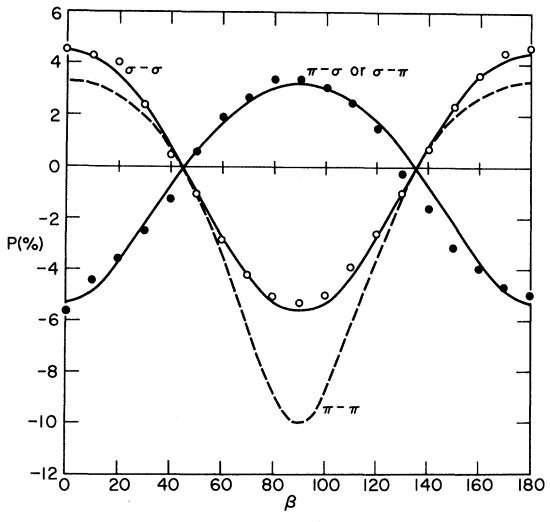

FIG. 13. Polarization diagrams for the 460-nm emission at LNT in NaCl : Pb^{2+} with [100] excitation and [001] observation.

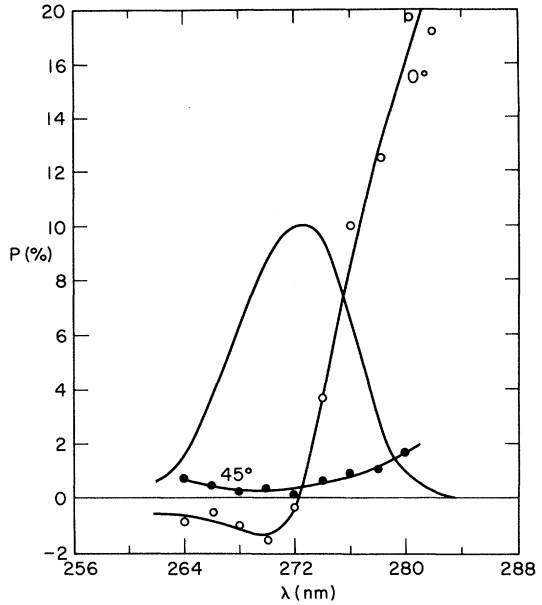

FIG. 14. Polarization and excitation spectra for the 340-nm emission at LNT in KCl : Pb^{2+}.

The polarization properties of the emission band are essentially independent of emission wavelength for both quenched and aged crystals. The dependence of polarization on the excitation wavelength across the *A* band is shown in Fig. 14 at LNT for crystal azimuths of 0° and 45°. Qualitatively the behavior is similar to that for the 315-nm emission in NaCl : Pb. However, the 45° variation is much smaller and remains positive, and the 0° variation does not increase as extensively on the high-energy side. Thus only two regions of distinct polarization character are observed, and only on the low-energy side is the polarization degree of sufficient magnitude to measure angular variation with accuracy. The azimuthal dependence for ⟨100⟩ cut crystals excited on the high- and low-energy side of the *A* band is qualitatively similar to the corresponding results in NaCl : Pb. The more revealing ⟨110⟩ perpendicular measurements are shown in Fig. 8

at RT and LNT. The polarization for KCl: Pb has only a small dependence on the polarizer angle β as contrasted with NaCl: Pb. Consulting Table II we again see that for tetragonal oscillators the expected polarization is independent of β. The solid curves in Fig. 8 are plots of the function from Table II corresponding to orthorhombic centers but the variation with β is so small for KCl: Pb that the explicit form cannot be accurately determined. In any case this result suggests the dominant presence of tetragonal centers in KCl: Pb.

IV. DISCUSSION AND CONCLUSION

As mentioned in the Introduction, all previous measurements of optical polarization yielded tetragonal symmetry. This suggests perturbations by next-nearest-neighbor vacancies if vacancies are the origin of the low symmetry, as suggested by the Dutch[11] and Russian[16-18] workers. Our measurements indicate the presence of centers with both tetragonal and orthorhombic symmetry, with the latter sites being more prevalent in NaCl: Pb than in KCl: Pb. If vacancies are responsible, then this implies a relatively greater population of nearest-neighbor sites in NaCl. This is consistent with Watkins's results[19] on KCl: Mn and NaCl: Mn using EPR, which also showed that orthorhombic complexes were more plentiful in NaCl than in KCl. The origin of the low symmetry as due to vacancies has been questioned by the Japanese investigators. Fukuda[12] in particular has always considered the dynamical Jahn-Teller effect (DJTE) as the origin of the anisotropy. Zazubovich[20] has lately come to this conclusion also. Recently, however, Fukuda[14] found it necessary to include the effects of vacancies along with the DJTE in order to explain the complex polarization properties of KI: Sn. Only by using nn vacancies could the data be qualitatively explained. It should be noted here that requiring the perturbing vacancies to be nearest neighbor is in conflict with the criterion of Dreyfus[21] for the relative stability of nearest-neighbor and next-nearest-neighbor sites. If the radius of the impurity is smaller than that of the cation which it replaces, then the next-nearest-neighbor complexes should be dominant.

The appearance of orthorhombic symmetry in our results cannot be accounted for purely on the basis of the DJTE. On the other hand the complexity of the NaCl: Pb polarization spectra and their low degree of polarization are difficult to explain purely on the basis of perturbing vacancies. Thus a possible conclusion might be that both effects are present. A theoretical analysis of the DJTE in these systems would be necessary in order to determine more exactly the relative importance of the two effects. Nevertheless, from the evidence of both orthorhombic and tetragonal symmetry it is tempting to conclude that two types of complexes with differing symmetry are present.

We have found that the 380- and 460-nm emission centers in NaCl: Pb are oriented along the crystal $\langle 111 \rangle$ axis. The 380-nm emission is the first to appear during aging with the 460-nm band appearing later. The behavior of the 380-nm band is consistent with the Cook and Dryden model for the first stage of aggregation as a trimer of dipoles in a hexagon arrangement in the $\{111\}$ plane. If there is sufficient overlap of the sp wave functions of the Pb^{+2} ions, then the excitation energy is shared equally by all three Pb ions in the complex. The optical axis of such a system could be $\langle 111 \rangle$. Such a molecular-orbital model would be a complicated extension of Sugano's model[6] for the isolated center as a mixture of the Pb and the six halide atomic orbitals. Extending this concept to higher aggregates becomes difficult to justify since the Pb ions become separated by considerable distances. This is particularly true for Dryden's and Harvey's heptamer model[7] for the 460-nm emission band. Conclusions from our study concerning the origin of the 460-nm emission band are not as well established as for the 315- and 380-nm bands. According to the above model, the 460-nm band should be dominant in aged high-concentration crystals, but as mentioned previously this is not always true. The relevance of the DJTE to these aggregates has not yet been treated, due to the complexity of the problem. Certainly the analysis[6,12,13] carried out for octahedrally coordinated s^2 centers would not apply in this case.

---

†This work supported by the U.S. Atomic Energy Commission under Contract No. AT-(40-1)-3677.

*Present address: Naval Research Laboratory, Washington, D.C.

[1]J. Quin, B. A. W. Redfern, and P. L. Pratt, Proc. Brit. Ceram. Soc. 9, 35 (1967).

[2]J. S. Cook and J. S. Dryden, Australian J. Phys. 13, 260 (1960); Proc. Phys. Soc. London 80, 479 (1962).

[3]J. H. Schulman, R. J. Ginther, and C. C. Klick, J. Opt. Soc. Am. 40, 854 (1950).

[4]A. Fukuda, Sci. Light 13, 64 (1964).

[5]F. Seitz, J. Chem. Phys. 6, 150 (1938).

[6]H. Kamimura and S. Sugano, J. Phys. Soc. Japan 14, 1612 (1959).

[7]J. S. Dryden and G. S. Harvey, J. Phys. C 2, 603 (1969).

[8]C. C. Klick and W. D. Compton, J. Phys. Chem. Solids 7, 170 (1958).

[9]N. W. Luschik and C. B. Luschik, Opt. i Spectroskopiya 8, 839 (1960) [Opt. Spectry (USSR) 8, 441 (1960)].

[10]S. G. Zazuborich, N. E. Lushchik, and C. B. Lushchik, Opt. i Spectroskopiya 15, 381 (1969) [Opt. Spectry. (USSR) 15, 203 (1969)].

[11]P. Koeze and J. Volger, Physica 37, 467 (1967).

[12]A. Fukuda, S. Marishima, T. Mabuchi, and R. Onaka, J. Phys. Chem. Solids 28, 1763 (1967).

[13]Y. Toyozawa and M. Inoue, J. Phys. Soc. Japan 21, 1663 (1966).
[14]A. Fukuda, Phys. Rev. Letters 21, 314 (1971).
[15]The expressions for ⟨100⟩ cut crystals were first reported by C. D. Clark, G. W. Maycraft, and E. W. J. Mitchell, J. Appl. Phys. 33, 378 (1962).
[16]C. B. Lushchik, J. Luminescence 1, 594 (1970).
[17]S. G. Zazubovich, N. E. Lushchik, and C. B. Lushchik, Izv. Acad. Nauk. SSSR 27, 656 (1963).
[18]S. G. Zazubovich and T. A. Kuketaev, Inst. Fiz. i Astron. Akad. Nauk. Est. SSSR 31, 190 (1966).
[19]G. D. Watkins, Phys. Rev. 113, 79 (1959).
[20]S. G. Zazubovich, Phys. Status Solidi 38, 119 (1970).
[21]R. W. Dreyfus, Phys. Rev. 121, 1675 (1961).

PHYSICAL REVIEW B VOLUME 5, NUMBER 2 15 JANUARY 1972

Hartree-Fock Band Structure and Optical Gap in Solid Neon and Argon

L. Dagens and F. Perrot
Commissariat à l'Energie Atomique, Centre d'Etudes de Limeil, B.P. No. 27-94, Villeneuve St. Georges, France
(Received 21 June 1971)

A method closely related to the classical augmented-plane-wave (APW) method is developed which treats in a nearly exact way the Hartree-Fock exchange in the case of crystals having deeply bound and filled valence bands. Band-structure calculations have been performed for solid neon and argon. The main conclusions of Lipari and Fowler for argon are confirmed: a too large gap which proves the influence of correlation in these insulators, large valence bands, and change in the shift between conduction bands without significant modification of their internal structure. Yet, we note that we found a smaller separation between s and d bands than Lipari and Fowler. The value of the Hartree-Fock energy gap is physically related to the experimental one in terms of the correlation energies involved in a transition from a localized valence state to an extended conduction state. Using atomic correlation values for the valence state and previous results for the polarization in solid rare gases, a good qualitative agreement is found.

I. INTRODUCTION

Different band-structure calculations on solid neon and argon have been performed during the last ten years paralleling the progress in experimental measurements. Knox and Bassani,[1] using a perturbation approximation to the orthogonalized-plane-wave (OPW) method, and two years later Mattheiss,[2] using the augmented-plane-wave (APW) method, have given the dispersion curves $E(k)$ for argon. These authors introduced the exchange potential by means of Slater's free-electron approximation. Their results were in qualitative agreement with experiment, though there were important quantitative differences.

The band structures of Ne, Ar, Kr, and Xe can also be found in a paper by Rössler.[3] The calculation for Ar up to Xe was based on the relativistic formulation of the Green's-function method, but was nonrelativistic for neon. The exchange was also taken into account by an approximate local potential, and the constant potential outside the "muffin tin" was chosen to obtain the experimental value of the gap between conduction and valence bands. The general features of the band structure of Ar were similar to those found in previous calculations.

The problem of the band structure of Ar has been recently considered by Lipari and Fowler.[4] Two types of new OPW calculations were made: a Hartree-Fock (HF) calculation with the exchange potential treated in a nearly exact manner, and a calculation where the correlations were included by a rather complicated procedure. The only agreement between the HF calculation and the previous results was the internal structure of the bands. But the energy gap found by Lipari and Fowler is much larger than previously calculated gaps and experimental gaps. Similarly, the separation between s and d bands is larger in the HF case, and the valence band is wider. Finally, the second calculation of Lipari and Fowler proved that the influence of correlations is very strong.

Thus the situation is that the gap, as calculated by Knox and Bassani and then by Mattheiss with statistical exchange, is in better agreement with experiment than the nearly exact HF gap of Lipari and Fowler. To explain this fact, we note that the comparison between the optical gap and difference of eigenvalues calculated in a statistical exchange potential is incorrect since, in this case, Koopmans's theorem fails. Slater[5] has pointed out that Koopmans's corrections are certainly significant when the optical transition occurs from an atomic-like localized state to an extended crystal state. It can be expected that a calculation with Kohn and Sham's statistical exchange and Koopman's correc-